IEEE Access
Multidisciplinary | Rapid Review | Open Access Journal

Received October 10, 2018, accepted November 5, 2018, date of publication December 19, 2018,
date of current version January 7, 2019.

Digital Object Identifier 10.1109/ACCESS.2018.2886656

Cooperative NOMA System With Virtual Full Duplex User Relaying

QIAN YU LIAU, (Student Member, IEEE), AND CHEE YEN LEOW, (Member, IEEE)
Wireless Communication Centre, School of Electrical Engineering, Faculty of Engineering, Universiti Teknologi Malaysia, Johor Bahru 81310, Malaysia

Corresponding author: Chee Yen Leow (bruceleow@utm.my)

This work was supported in part by H2020-MSCA-RISE-2015 under Grant 690750, in part by the Ministry of Education Malaysia under Grant 4F818, Grant 07085, and Grant 4J210, and in part by the Universiti Teknologi Malaysia under Grant 19H58 and Grant 04G37.

ABSTRACT Cooperative non-orthogonal multiple access (NOMA) system employs user relaying to enhance performance. Although full-duplex (FD) user relaying scheme does not incur additional bandwidth for relaying, the imperfect self-interference cancellation degrades the performance significantly. Alternatively, a virtual full-duplex (VFD) user relaying scheme can be used. In this paper, we study a cooperative NOMA system in cognitive radio scenario using VFD relaying scheme, where two half-duplex (HD) secondary users take turn to relay message of a primary user with decode-and-forward (DF) strategy. First, we derive the closed-form and asymptotic expressions of the outage probability and ergodic rate of the users. Then, we demonstrate the outage probability, ergodic rate, and ergodic sum rate performance of the proposed scheme using Monte Carlo simulations. We also provide a comprehensive comparison between the proposed VFD user relaying and existing FD and HD user relaying in orthogonal multiple access and NOMA systems. The simulation results verify the analytical results and demonstrate the advantages of the proposed VFD user relaying over existing schemes.

INDEX TERMS Non-orthogonal multiple access (NOMA), decode-and-forward (DF), virtual full-duplex relaying, user relaying, cognitive radio scenario.

I. INTRODUCTION

The upcoming 5th Generation (5G) system is expected to support the massive Internet of Things (IoT) use case, where large number of IoT devices will be connected to the internet [1], [2]. Conventional orthogonal multiple access (OMA) technique is not able to address the massive IoT use case without consuming excessive channel resource, due to the fact that each connection requires an orthogonal channel. Non-orthogonal multiple access (NOMA) technique is a promising multiple access technique to provide higher spectral efficiency by multiplexing signals of multiple users in different power levels using superposition coding [3], [4]. For instance, in a network with two users, the user with stronger channel gain can perform successive interference cancellation (SIC) to decode its own message after decoding the message of the user with weaker channel. With the prior information, the strong user can help as a decode-and-forward (DF) relay to forward the information for the weak user. This user relaying scheme in NOMA system is also known as cooperative NOMA system [5].

References [5]–[7] studied the cooperative NOMA system with half-duplex (HD) relay, where a dedicated time slot or channel is required for relaying phase. Reference [5] studied the impact of user pairing and analyzed the outage probability and diversity order. References [6] and [7] analyzed the achievable average rate and the outage probability of HD user relaying for independent Rayleigh fading channels, respectively. However, the HD user relaying requires additional bandwidth and reduces spectral efficiency of the system because the relaying user isolates the transmit and receive signals in two orthogonal time slots or frequency channels.

Full duplex (FD) user relaying is one of the promising solutions to avoid additional bandwidth being used for relaying [8]–[10]. Unlike the HD relay, the FD relay transmits and receives signals concurrently in the same frequency. However, the transmit signal of FD relay imposes significant amount of self-interference to its received signal. Ideally, the FD relay can remove the self-interference perfectly since the transmit signal is known by the FD relay. But, the transmit signal of FD relay saturates the analog-to-digital converter (ADC) of receiver since the power of transmit signal is much larger than its desired received signal [11]. Hence, a perfect self-interference cancellation is impossible due to

the large power difference between the transmit and desired received signals. As a result, the performance of FD relay is degraded by the residual self-interference. Reference [8] analyzed the outage probability of the FD user relaying with imperfect self-interference cancellation. Reference [9] considered the impact of power split factors to the outage probability and the ergodic sum rate of the FD user relaying with imperfect self-interference cancellation. Reference [10] compares performance of HD user relaying and FD user relaying with imperfect self-interference cancellation in terms of outage probability, ergodic rate, and energy efficiency.

Alternatively, a virtual full-duplex (VFD) technique known as the distributed version of FD relay can recover the loss of spectral efficiency using only HD relay [12]. A pair of HD relays receive and transmit signals successively to imitate the operation of FD relay [13]. The physical separation between the two HD relays eliminates the receiver ADC saturation problem. In [14], two HD relays with amplify-and-forward (AF) strategy are scheduled to receive and transmit signals alternately in a cognitive radio scenario. In the cognitive radio scenario, the users are categorized as primary user and secondary user according to their quality-of-service (QoS) requirement [15], unlike the conventional cooperative NOMA system that order users based on their channel conditions. The proposed scheme in [14] is able to serve a pair of users with lower outage probability and higher ergodic rate than a FD relay with perfect self-interference cancellation [14]. However, the DF based cooperative user relaying using VFD technique still remains unexplored.

This paper studies a cooperative NOMA system using VFD technique in a cognitive radio scenario (referred to VFD-NOMA hereinafter). In the proposed VFD-NOMA, a pair of secondary users are scheduled to receive message from a base station and take turn to relay message of a primary user with DF strategy. The closed-form expressions of the outage probability and ergodic rate of users are derived. We provide a comprehensive comparison between the proposed VFD-NOMA and the existing FD and HD user relaying schemes in NOMA and OMA systems in terms of outage probability, ergodic outage rate, ergodic rate and ergodic sum rate. Simulation results show that the proposed VFD-NOMA attains significant improvement compared to the existing schemes.

The rest of the paper is organized as follows: Section II describes the system model. Section III presents the analytical results on outage probability and ergodic rate of users. Section VI provides the simulation results. Finally, Section V concludes the paper.

II. SYSTEM MODEL

In conventional cooperative NOMA system, the users are ordered based on their channel conditions. Unlike the conventional cooperative NOMA system, we categorize the users based on their priority of services [15]. For example, a user making a voice call is given higher priority to achieve his QoS than a user surfing a website. We consider a cooperative

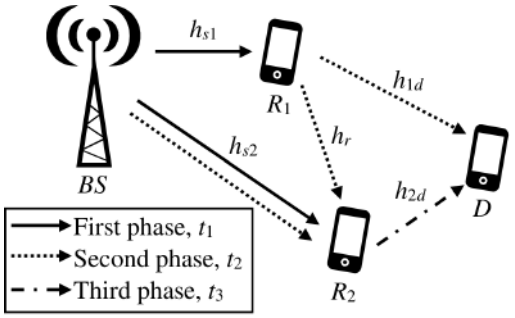

FIGURE 1. A cognitive radio scenario, where a primary user *D* is given higher priority to achieve its quality-of-service (QoS) than a pair of secondary users, i.e., R_1 and R_2. The pair of secondary users using virtual full-duplex (VFD) user relaying to assist the primary user successively.

NOMA system using VFD user relaying, which consists of a base station (BS), two secondary users, i.e., R_1 and R_2, and a primary user (D) as shown in Figure 1. We assume perfect SIC receiver[1] and each user is equipped with a single antenna. There is no direct link between BS and D due to physical obstruction or heavy shadowing. R_1 and R_2 are scheduled to receive signal from BS and relay signal to D alternately in HD mode using DF strategy as shown in Figure 1. The channel coefficients between nodes are known as follows: h_{si} denotes the channels between BS and R_i, h_r denotes the channel between R_1 and R_2, and h_{id} denotes the channels between R_i and D, where $i = \{1, 2\}$. All the channels experience independent and identically quasi-static Rayleigh fading and all the channels are reciprocal. In the following, signal model of VFD-NOMA and signal-to-interference-and-noise-ratio (SINR) and signal-to-noise-ratio (SNR) at the users are provided.

A. SIGNAL MODEL

The transmission protocol of the proposed VFD-NOMA is divided into three phases. During the first phase, BS broadcasts a superimposed mixture, $x_s(t_1)$ to R_1 and R_2 such that

$$x_s(t_1) = \sqrt{\alpha P_s}\, x_r(t_1) + \sqrt{\beta P_s}\, x_d(t_1), \tag{1}$$

containing messages $x_r(t_1)$ for R_1 and $x_d(t_1)$ for D, where α and β denote the power split factors of secondary user and primary user, respectively, and P_s is the transmission power of BS. Note that $\alpha + \beta = 1$ and $\alpha < \beta$ as D is to be served with a higher priority than R_i as in [15]. The received signals at R_1 and R_2 are given by

$$y_{r1}(t_1) = h_{s1}\, x_s(t_1) + w_1, \tag{2}$$
$$y_{r2}(t_1) = h_{s2}\, x_s(t_1) + w_2, \tag{3}$$

respectively, where w_i is the noise at R_i and follows $w_i \sim \mathcal{CN}(0, \sigma^2)$. R_1 decodes its own message, $x_r(t_1)$ after decoding and removing $x_d(t_1)$ using SIC technique. At the same time, R_2 also decodes $x_d(t_1)$, so it can remove the inter-user interference signal from R_1 in next phase.

[1] Imperfection of SIC can result in performance degradation [16].

During the second phase, R_1 relays the decoded $x_d(t_1)$ to D, and the received signal at D is given by

$$y_d(t_2) = \sqrt{P_r}\, h_{1d}\, x_d(t_1) + w_d, \tag{4}$$

where P_r is the transmission power of R_i, w_d is the noise at D that follows $w_d \sim \mathcal{CN}(0,\ \sigma^2)$. Simultaneously, BS transmits a new superimposed mixture,

$$x_s(t_2) = \sqrt{\alpha\, P_s}\, x_r(t_2) + \sqrt{\beta\, P_s}\, x_d(t_2) \tag{5}$$

to R_2, and the received signal at R_2 is given by

$$y_{r2}(t_2) = h_{s2}\, x_s(t_2) + \sqrt{P_r}\, h_r\, x_d(t_1) + w_2. \tag{6}$$

R_2 can remove the inter-user interference signal, $\sqrt{P_r}\, h_r\, x_d(t_1)$ in (6) after estimating $\sqrt{P_r}\, h_r$, using $x_d(t_1)$ obtained previously. After removing the inter-user interference signal, the received signal at R_2 can be rewritten as

$$y^*_{r2}(t_2) = h_{s2}\, x_s(t_2) + w_2. \tag{7}$$

Then, R_2 decodes $x_d(t_2)$ and its own message, $x_r(t_2)$ using SIC technique.

Finally, during the third phase, R_2 relays decoded $x_d(t_2)$ to D, and the received signal at D is given by

$$y_d(t_3) = \sqrt{P_r}\, h_{2d}\, x_d(t_2) + w_d. \tag{8}$$

B. SINR AND SNR

Based on SIC technique, R_i decodes $x_d(t_j)$ first, where $j = \{1,\ 2\}$, and the SINR when R_i detects $x_d(t_j)$ is given as

$$\gamma_{ri,d} = \frac{\beta\, P_s\, |h_{si}|^2}{\alpha\, P_s\, |h_{si}|^2 + \sigma^2}. \tag{9}$$

Then, conditioned on successfully decoding of $x_d(t_j)$, R_i subtracts $x_d(t_j)$ from its received signal, $y_{ri}(t_j)$ and detect its own message, $x_r(t_j)$. The SNR to detect $x_r(t_j)$ at R_i is given as

$$\gamma_{ri} = \frac{\alpha\, P_s\, |h_{si}|^2}{\sigma^2}. \tag{10}$$

When R_i relays the decoded $x_d(t_j)$ to D, the SNR to detect $x_d(t_j)$ at D is given as

$$\gamma_{di} = \frac{P_r\, |h_{id}|^2}{\sigma^2}. \tag{11}$$

III. PERFORMANCE ANALYSIS

In this section, outage probability and ergodic rate of users in proposed VFD-NOMA are investigated. Outage probability is an important metric to evaluate the reliability of transmission system when the transmitter adopts fixed rate in accordance with QoS requirement of user. Meanwhile, the ergodic rate is used to evaluate the achievable rate of user when the transmitter adjusts transmission rate according to wireless channel variations.

TABLE 1. Outage events for each stream in the proposed VFD-NOMA.

Outage Events	Descriptions
A_1	R_1 fails to decodes $x_d(t_1)$
A_2	R_1 fails to decodes $x_r(t_1)$
B_1	R_2 fails to decodes $x_d(t_1)$ and $x_d(t_2)$
B_2	R_2 fails to decodes $x_r(t_2)$
C_1	D fails to decodes $x_d(t_1)$ from R_1
C_2	D fails to decodes $x_d(t_2)$ from R_2

A. OUTAGE PROBABILITY OF USERS

In this part, we investigate outage probability of R_i and outage probability of D. Let T_r and T_d be the predetermined target rate in accordance with QoS requirements of R_i and D, respectively. For each data stream, it is defined that the outage event occurs when the achievable rate is smaller than the corresponding target rate. Table 1 lists out the outage events of each stream. During the first phase, in order to remove the inter-user interference in the second phase, R_2 decodes $x_d(t_1)$. Event B_1 denotes event of R_2 fails to decode $x_d(t_1)$ and $x_d(t_2)$, because we assume that h_{s2} is quasi-static over the transmission period.

Theorem 1: The closed-form expressions for outage probability of R_1 and R_2 are

$$\begin{aligned}\mathcal{O}_{R_1} &= 1 - \Pr[A_1^c]\ \Pr[A_2^c] \\ &= 1 - \exp\left(-\frac{(2^{T_d}-1)\,\sigma^2}{(1-\alpha\, 2^{T_d})P_s\,\lambda}\right) \\ &\quad \times \exp\left(-\frac{(2^{3T_r}-1)\,\sigma^2}{\alpha\, P_s\,\lambda}\right),\end{aligned} \tag{12}$$

and

$$\begin{aligned}\mathcal{O}_{R_2} &= 1 - \Pr[B_1^c]\ \Pr[B_2^c] \\ &= 1 - \exp\left(-\frac{(2^{T_d}-1)\,\sigma^2}{(1-\alpha\, 2^{T_d})P_s\,\lambda}\right) \\ &\quad \times \exp\left(-\frac{(2^{3T_r}-1)\,\sigma^2}{\alpha\, P_s\,\lambda}\right),\end{aligned} \tag{13}$$

where $\mathring{u}^c$ denotes the complementary event and the channel power gain, $|h_{si}|^2$ is assumed to be exponentially distributed random variables with parameters λ.

Proof of Theorem 1: Please refer to Appendix A.

Theorem 2: The closed-form expression for outage probability of D is

$$\begin{aligned}\mathcal{O}_D &= 1 - \Pr[A_1^c]\ \Pr[C_1^c]\ \Pr[B_1^c]\ \Pr[C_2^c] \\ &= 1 - \exp\left(-\frac{2\,\sigma^2\,(2^{3\,T_d}-1)}{(1-\alpha\, 2^{3T})P_s\,\lambda}\right) \\ &\quad \times \exp\left(-\frac{2\,\sigma^2\,(2^{3\,T_d}-1)}{P_r\,\lambda}\right).\end{aligned} \tag{14}$$

where the channel power gain, $|h_{id}|^2$ is exponentially distributed random variables with parameters λ.

Proof of Theorem 2: Please refer to Appendix B.

Remark 1: Theorem 1 in (12) and (13) indicate that the power split factor, α plays an important role in the outage probability at R_i. Based on the Theorem 1, when $\alpha = 2^{-T_d}$, R_1 fails to decode $x_d(t_1)$ and R_2 fails to decode $x_d(t_1)$ and $x_d(t_2)$. Moreover, when $\alpha = 0$, R_1 fails to decode $x_r(t_1)$ and R_2 fails to decodes $x_r(t_2)$. Therefore, the outage probability of R_i is 1, i.e., outage occurs at R_i, when $\alpha = \{0, 2^{-T_d}\}$. On the other hand, Theorem 2 in (14) also reveals that the outage probability of D is 1 when $\alpha = 2^{-3T_d}$. In addition, when $\alpha = 1$, the outage probability of D is 1 because $\beta = 0$ and R_i fails to decode $x_d(t_1)$ and $x_d(t_2)$. Therefore, the outage probability of D is 1 when $\alpha = \{2^{-3T_d}, 2^{-T_d}, 1\}$.

Based on (12), (13), and (14), when $\sigma^2 \to 0$, by using $\lim_{x\to\infty} \exp(-x) \approx 1 - x$, the asymptotic outage probability of R_1, R_2, and D are given by

$$\mathcal{O}_{R_1}^{\infty} = \frac{(2^{T_d} - 1)}{(1 - \alpha\, 2^{T_d}) P_s\, \lambda\, \rho} + \frac{(2^{3T_r} - 1)}{\alpha\, P_s\, \lambda\, \rho}, \tag{15}$$

$$\mathcal{O}_{R_2}^{\infty} = \frac{(2^{T_d} - 1)}{(1 - \alpha\, 2^{T_d}) P_s\, \lambda\, \rho} + \frac{(2^{3T_r} - 1)}{\alpha\, P_s\, \lambda\, \rho}, \tag{16}$$

and

$$\mathcal{O}_{D}^{\infty} = \frac{2\,(2^{3\,T_d} - 1)}{(1 - \alpha\, 2^{3T}) P_s\, \lambda\, \rho} + \frac{2\,(2^{3\,T_d} - 1)}{P_r\, \lambda\, \rho}, \tag{17}$$

respectively, where $\rho = \frac{1}{\sigma^2}$. Given diversity gain is defined as $d = -\lim_{\rho\to\infty} \frac{\log[\mathcal{O}^{\infty}(\rho)]}{\log\, \rho}$ [17], based on (15), (16), and (17), the diversity gain at R_1, R_2, and D are 1.

B. ERGODIC RATE OF USERS

In this part, we study the ergodic rates of R_1, R_2, and D. The instantaneous rate of R_1 is

$$C_{R_1} = \frac{1}{3}\, \log_2(1 + \gamma_{r1}), \tag{18}$$

conditioned on R_1 decodes $x_d(t_1)$ successfully, i.e., $\log_2(1 + \gamma_{r1,d}) \geq T_d$, where T_d is predetermined target rate of D. The instantaneous rate of R_2 is

$$C_{R_2} = \frac{1}{3}\, \log_2(1 + \gamma_{r2}), \tag{19}$$

conditioned on R_2 decodes $x_d(t_1)$ and $x_d(t_2)$ successfully, i.e., $\log_2(1 + \gamma_{r2,d}) \geq T_d$. The instantaneous rate of D is

$$C_D = \frac{1}{3}\, \log_2(1 + \min(\gamma_{r1,d},\, \gamma_{d1})) + \frac{1}{3}\, \log_2(1 + \min(\gamma_{r2,d},\, \gamma_{d2})), \tag{20}$$

respectively. A complete transmission of proposed VFD-NOMA requires three time slots, i.e., $TS = 3$. Throughout the three time slots, R_1 receives $x_r(t_1)$, R_2 receives $x_r(t_2)$, and D receives $x_d(t_1)$ and $x_d(t_2)$. Therefore, the pre-log factor of each stream, $\mu = \frac{1}{TS}$ in (18), (19), and (20) is $\frac{1}{3}$.

Theorem 3: The closed-form ergodic rate of R_i, $i = \{1,\, 2\}$, is

$$\overline{C}_{R_i} = -\frac{1}{3\, \ln 2}\, \exp\left(\frac{\sigma^2}{\alpha\, P_s\, \lambda}\right) \mathrm{Ei}\left(-\frac{\sigma^2}{\alpha\, P_s\, \lambda}\right), \tag{21}$$

where $\mathrm{Ei}\,(x) = \int_{-\infty}^{x} \frac{1}{t}\, \exp\,(t)\, dt$, $x < 0$, is the exponential integral function.

Proof of Theorem 3: Please refer to Appendix C.

Theorem 4: The asymptotic ergodic rate of D is

$$\overline{C}_D = \frac{2\, \log_2(\exp\,(1))}{3} \left\{ \exp\left(\frac{2\,\sigma^2}{\alpha\, P_s\, \lambda}\right) \mathrm{Ei}\left(-\frac{2\,\sigma^2}{\alpha\, P_s\, \lambda}\right) - \exp\left(\frac{2\,\sigma^2}{P_s\, \lambda}\right) \mathrm{Ei}\left(-\frac{2\,\sigma^2}{P_s\, \lambda}\right) \right\}. \tag{22}$$

Proof of Theorem 4: Please refer to Appendix D.

Remark 2: When $\alpha = 0$, $\overline{C}_{R_i} = 0$ bits/s/Hz, but D achieves its maximum ergodic rate. As mentioned in Remark 1, when $\alpha = 2^{-T_d}$, R_i fails to decode $x_d(t_1)$ and $x_d(t_2)$, therefore, $\overline{C}_{R_i} = 0$ bits/s/Hz and $\overline{C}_D = 0$ bits/s/Hz.

Based on (21), when $\sigma^2 \to 0$, by using $\lim_{x\to\infty} \exp(-x) \approx 1 - x$ and $\mathrm{Ei}(-x) \approx \ln(x) + C$ [18, eq. (8.212.1)], where $C = 0.5772$ is Euler constant, the asymptotic ergodic rate of R_i is given by

$$\overline{C}_{R_i}^{\infty} = -\frac{1}{3\, \ln 2} \left(1 + \frac{\sigma^2}{\alpha\, P_s\, \lambda}\right) \left(\ln\left(\frac{\sigma^2}{\alpha\, P_s\, \lambda}\right) + C\right). \tag{23}$$

Given spatial multiplexing gain is defined as $r = -\lim_{\rho\to\infty} \frac{\log\left[\overline{C}^{\infty}(\rho)\right]}{\log\, \rho}$ [17], based on (22) and (23), the spatial multiplexing gain of R_i and D are $\frac{1}{3}$ and 0, respectively.

Corollary 3: Based on (21) and (22), the ergodic sum rate of proposed VFD-NOMA is

$$\begin{aligned} \overline{C}_T &= \overline{C}_{R_1} + \overline{C}_{R_2} + \overline{C}_D \\ &= \frac{2\, \log_2(\exp\,(1))}{3}\, \exp\left(\frac{2\,\sigma^2}{\alpha\, P_s\, \lambda}\right) \mathrm{Ei}\left(-\frac{2\,\sigma^2}{\alpha\, P_s\, \lambda}\right) \\ &\quad - \frac{2\, \log_2(\exp\,(1))}{3}\, \exp\left(\frac{2\,\sigma^2}{P_s\, \lambda}\right) \mathrm{Ei}\left(-\frac{2\,\sigma^2}{P_s\, \lambda}\right) \\ &\quad - \frac{2}{3\, \ln 2}\, \exp\left(\frac{\sigma^2}{\alpha\, P_s\, \lambda}\right) \mathrm{Ei}\left(-\frac{\sigma^2}{\alpha\, P_s\, \lambda}\right). \end{aligned} \tag{24}$$

IV. SIMULATION RESULTS

In this section, we provide simulation results to validate the analytical results. We also compare the performance of the proposed VFD-NOMA with existing schemes in terms of outage probability, ergodic rate and ergodic sum rate. The system parameters in the simulation are stated in Table 2.

A. SCHEMES FOR COMPARISON

In this paper, comparisons of the proposed VFD-NOMA with four existing schemes are provided. The existing schemes used for comparison are cooperative NOMA system with half-duplex technique (HD-NOMA) [6] and full-duplex technique (FD-NOMA) [9] and cooperative OMA system with half-duplex technique (HD-OMA) [13] and full-duplex technique (FD-OMA) [19]. Unlike the proposed VFD-NOMA, the existing schemes for comparison consist of only one

TABLE 2. System parameters of Monte Carlo simulations.

System Parameters	Values
No. of channel realizations	2×10^6
Channel variance, λ	1^2
SNR	$1/\sigma^2$
Power split factors, $(\alpha,\ \beta)$	$(0.05,\ 0.95)$
Transmission power of BS, P_s	1 W
Transmission power of BS in cooperative OMA, $P_{s,o}$	0.5 W
Transmission power of R_i, P_r	0.5 W
Self-interference cancellation factor, K	0.2

TABLE 3. Outage events for each stream in the comparable schemes.

Outage Events	Descriptions
V_1	R fails to decodes $x_d(t_1)$ and $x_d(t_2)$
V_2	D fails to decodes $x_d(t_1)$ and $x_d(t_2)$ from R
V_3	R fails to decodes $x_r(t_1)$ and $x_r(t_2)$

secondary user, R. R acts as a relay to assist the primary user, D. Table 3 lists out the outage events for each stream in the comparable schemes.

In HD-NOMA and FD-NOMA, BS broadcasts $x_s(t_1)$ in (1) and $x_s(t_2)$ in (5) to R in two different time slots. When $P_s = 1$ W, it is assumed that BS allocates 0.05 W and 0.95 W to $x_r(t_j)$ and $x_d(t_j)$, respectively, where $j = \{1,\ 2\}$. On the other hand, in HD-OMA and FD-OMA, BS broadcasts $x_r(t_1)$, $x_r(t_2)$, $x_d(t_1)$, and $x_d(t_2)$ in orthogonal time slots, i.e., time division multiple access (TDMA), with an equal power allocation. For the sake of fairness in total transmission power, the transmission power of BS with OMA, $P_{s,o} = P_s/2$, i.e., 0.5 W. More detailed scheme descriptions of comparable schemes can be found in Appendix E. Refer to Tables 4 and 5 in Appendix E, the required time slots for a complete transmission, TS in the existing HD-NOMA, FD-NOMA, HD-OMA, and FD-OMA are 4, 2, 6, and 4, respectively. For each scheme, the pre-log factor of each stream, μ varies inversely with TS, i.e., $\mu = 1/TS$. The following curves for comparisons of HD-NOMA, FD-NOMA, HD-OMA, and FD-OMA are from simulation expressions in [6], [9], [13], and [19], respectively.

B. RESULTS OF OUTAGE PROBABILITY

Figure 2 shows the outage probability of secondary users R_1 and R_2 in the proposed VFD-NOMA and secondary user R in the existing schemes. Based on Theorem 1, the outage probability of R_1 and R_2 in (12) and (13), respectively, are identical because h_{s1} and h_{s2} are independent and identically distributed. The exact analytical curves for outage probability of R_1 and R_2 when $T = 0.1$ and 1.0 bits/s/Hz are plotted and shown to precisely match the Monte Carlo simulation results. From the figure, the proposed VFD-NOMA with higher μ achieves lower outage probability than the existing HD-NOMA, i.e., 1/3 versus 1/4. Conversely, due to the residual self-interference, FD-NOMA with the highest μ, i.e., 1/2, among all the schemes undergoes the highest outage probability. Note that the allocated power of BS to $x_r(t_j)$ in cooperative OMA system is higher than the cooperative

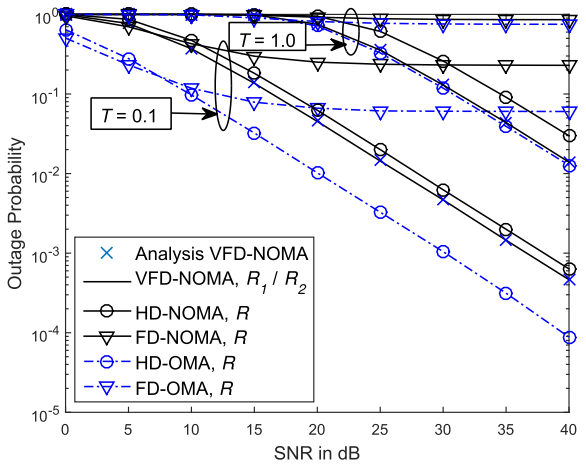

FIGURE 2. Outage probability of secondary users R_1, R_2, and R in various schemes when $T_r = T_d = T$.

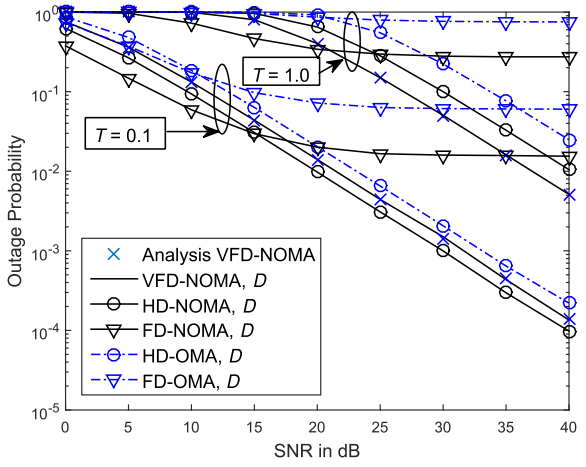

FIGURE 3. Outage probability of primary user D in various schemes when $T_r = T_d = T$.

NOMA system, i.e., 0.5 W versus 0.05 W. As a result, the existing HD-OMA achieves lower outage probability than the proposed VFD-NOMA and HD-NOMA. With the same reason, the existing FD-OMA achieves lower outage probability than the existing FD-NOMA, and the proposed VFD-NOMA when SNR $<$ 20 dB.

Figure 3 shows the outage probability of primary user D in the proposed VFD-NOMA and existing schemes. The exact analysis curves for outage probability of D in (14) is plotted and it precisely matches the simulation curves of the proposed VFD-NOMA when $T = 0.1$ and 1.0 bits/s/Hz. From the figure, the proposed VFD-NOMA with lower μ outperforms FD-NOMA at high SNR regime, i.e., SNR $\geq$ 20 dB. This is because the residual self-interference limits the performance of FD-NOMA at high SNR. Meanwhile, the proposed VFD-NOMA with higher μ achieves lower outage probability than HD-NOMA, HD-OMA, and FD-OMA. From Tables 1 and 3, the outage events of the proposed VFD-NOMA with R_1 and R_2 is more than HD-NOMA with only one R. As a result, the proposed VFD-NOMA

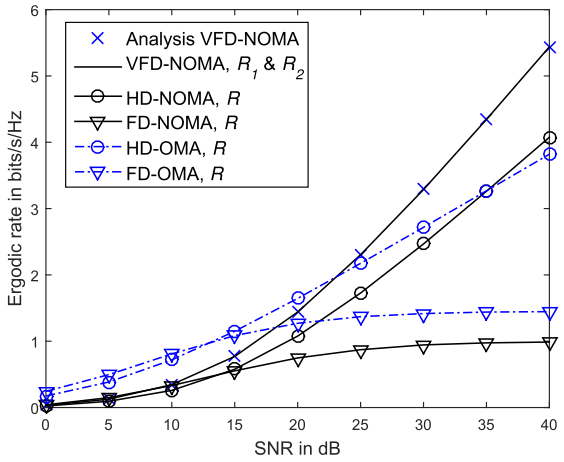

FIGURE 4. Ergodic rate of secondary users R_1, R_2, and R in various schemes when $T_d = 1$ bits/s/Hz.

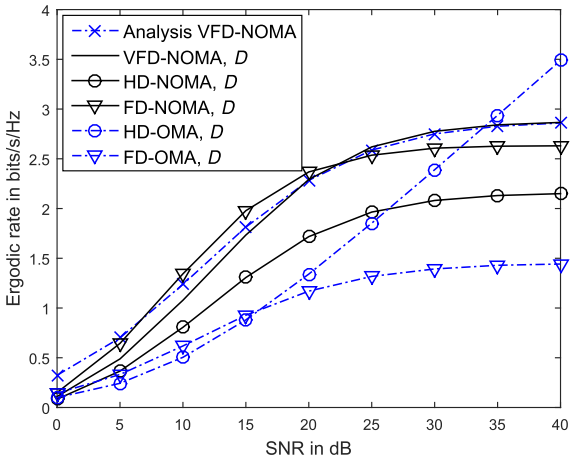

FIGURE 5. Ergodic rate of primary user D in various schemes when $T_d = 1$ bits/s/Hz.

has a higher outage probability compared to the existing HD-NOMA when T is low, i.e., $T = 0.1$ bits/s/Hz. Meanwhile, with higher μ, HD-NOMA and FD-NOMA attain lower outage probability compared to HD-OMA and FD-OMA, respectively. Note that the allocated power of BS to $x_d(t_j)$ in cooperative NOMA systems is also higher than the cooperative OMA systems, i.e., 0.95 W versus 0.5 W.

C. RESULTS OF ERGODIC RATE

Figure 4 shows the ergodic rate of secondary users R_1 and R_2 in the proposed VFD-NOMA and secondary user R in existing schemes. The sum of exact analytical ergodic rate curve for R_1 and R_2 in the proposed VFD-NOMA is plotted and it closely matches the simulation curve of the proposed VFD-NOMA. From the figure, the proposed VFD-NOMA attains higher ergodic rate than the comparable schemes when SNR $\geq$ 25 dB. This is because generally the proposed VFD-NOMA has a higher μ than HD-NOMA, HD-OMA, and FD-OMA. At the same time, the residual self-interference of FD-NOMA and FD-OMA degrade their ergodic rates significantly at high SNR. Note that the allocated power of BS to $x_r(t_j)$ in cooperative NOMA system is lower than the cooperative OMA system, i.e., 0.05 W versus 0.5 W. Therefore, the proposed VFD-NOMA achieves lower ergodic rate than HD-OMA and FD-OMA when SNR $<$ 25 dB and 20 dB, respectively. Similarly, HD-NOMA and FD-NOMA achieve lower ergodic rate than HD-OMA and FD-OMA, respectively. However, HD-NOMA with higher μ than HD-OMA achieves higher ergodic rate when SNR $\geq$ 35 dB, i.e., 1/4 versus 1/6.

Figure 5 shows the ergodic rate of primary user D in the proposed VFD-NOMA and existing schemes. The asymptotic ergodic rate of D in (14) is plotted and it matches well the simulation curve of the proposed VFD-NOMA when SNR $\geq$ 20 dB. The proposed VFD-NOMA with higher μ achieves higher ergodic rate than HD-NOMA, HD-OMA, and FD-OMA. Note that due to the residual self-interference,

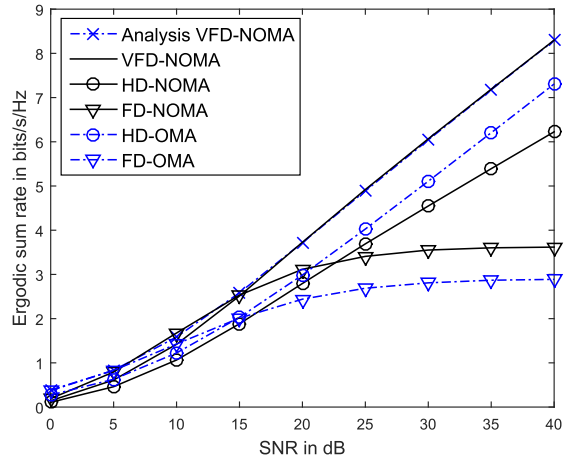

FIGURE 6. Ergodic sum rate of secondary users and primary user in various schemes when $T_d = 1$ bits/s/Hz.

FD-NOMA with higher μ than the proposed VFD-NOMA attains lower ergodic rate than proposed VFD-NOMA when SNR $\geq$ 25 dB. Meanwhile, HD-OMA achieves higher ergodic rate than the proposed VFD-NOMA and HD-NOMA when SNR $\geq$ 35 dB and 25 dB, respectively. This is because in cooperative NOMA systems, secondary user R_i or R have to perform SIC and the SINR when R_i or R decode $x_d(t_j)$ limit the ergodic rate at high SNR when target rate T_d is high.

Figure 6 shows the ergodic sum rate of proposed VFD-NOMA and the existing schemes. The ergodic sum rate analysis in (24) is plotted and it matches the simulation curve when SNR $\geq$ 20 dB. The proposed VFD-NOMA achieves a higher ergodic sum rate than HD-NOMA because μ of proposed VFD-NOMA is higher than HD-NOMA, i.e., 1/3 versus 1/4. The proposed VFD-NOMA outperforms FD-NOMA when SNR $>$ 15 dB. The reason is that the residual self-interference in FD-NOMA degrades its performance at high SNR. When SNR $\geq$ 10 dB, the proposed VFD-NOMA achieves a higher ergodic sum rate than HD-OMA and

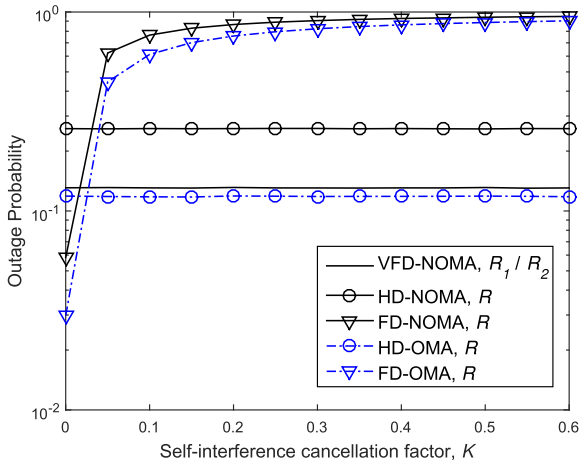

FIGURE 7. Outage probability of secondary users R_1, R_2, and R versus self-interference cancellation factor, K when SNR = 30 dB and $T_r = T_d = 1$ bits/s/Hz.

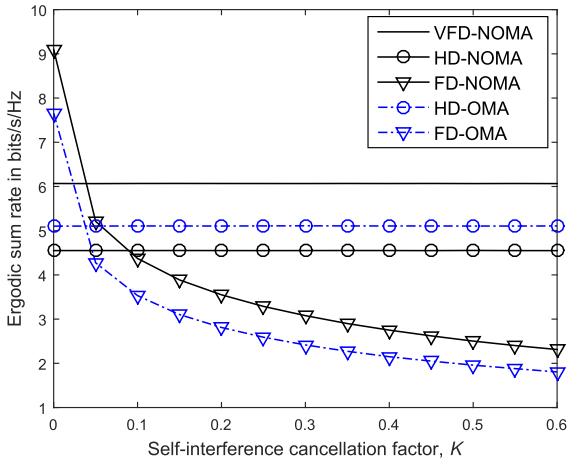

FIGURE 9. Ergodic sum rate of secondary users and primary user versus self-interference cancellation factor, K when SNR = 30 dB and $T_d = 1$ bits/s/Hz.

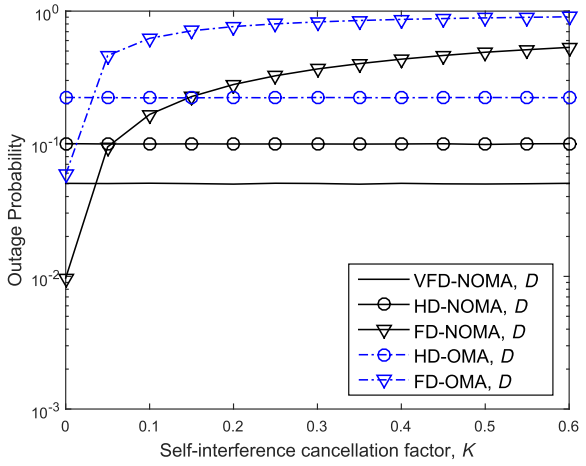

FIGURE 8. Outage probability of primary user D versus self-interference cancellation factor, K when SNR = 30 dB and $T_r = T_d = 1$ bits/s/Hz.

FD-OMA due to the higher μ of the proposed VFD-NOMA compared to HD-OMA and FD-OMA.

D. IMPACT OF SELF-INTERFERENCE CANCELLATION FACTOR, K

Figures 7, 8, and 9 show the impact of self-interference on outage probability of R, outage probability of D, and ergodic sum rate, respectively, when SNR = 30 dB and $T_r = T_d = 1$ bits/s/Hz. The self-interference cancellation factor, K shows the level of residual self-interference. For instance, $K = 0$ means perfect self-interference cancellation technique is adopted and no residual self-interference, and $K = 0.6$ means 40% of self-interference is canceled and 60% of self-interference remains. It is obvious that when $K \geq 0.05$, i.e., 5% of self-interference or more remains, the proposed VFD-NOMA outperforms FD-NOMA and FD-OMA in terms of outage probability of R, outage probability of D, and ergodic sum rate. Moreover, at $K = 0$, the proposed VFD-NOMA delivers a lower outage probability at D if compared to FD-OMA.

V. CONCLUSIONS

In this paper, we studied a cooperative NOMA system with VFD user relaying technique, where a pair of HD secondary users act as relays to serve a primary user alternately. The primary user is served with higher priority than the pair of secondary users. We first derived the closed-form expressions for outage probability and ergodic rate of users. Then, the analytical results are validated with simulation results. We also demonstrated the advantages of the proposed VFD-NOMA over the existing schemes. The performance of the secondary and primary users in the proposed VFD-NOMA are verified in terms of outage probability, ergodic rate and ergodic sum rate. From the simulation results, the proposed VFD-NOMA outperforms the existing schemes, i.e, HD-NOMA, FD-NOMA, HD-OMA, and FD-NOMA. This is mainly contributed by the perfect inter-user interference cancellation between the two secondary users. Furthermore, the pre-log factor of each stream in the proposed VFD-NOMA is higher than HD-NOMA, HD-OMA, and FD-OMA. The higher pre-log factor eventually provides better spectral efficiency to the users. Finally, the power split factors in NOMA schemes allow more flexibility in power allocation of messages compared to OMA schemes. As future work, the imperfect SIC receiver and adaptive power split factors can be further investigated.

APPENDIX

A. PROOF OF THEOREM 1

The outage probability of R_1 is given by

$$\mathcal{O}_{R_1} = 1 - \Pr[A_1^c]\,\Pr[A_2^c]. \tag{25}$$

Given probability density function (PDF) of $X = |h_{s1}|^2$ is $f_x(x) = \Pr[X > x] = \exp(-\frac{x}{\lambda})$, therefore, $\Pr[A_1^c]$ and $\Pr[A_2^c]$

are obtained as follows:

$$\begin{aligned}\Pr[A_1^c] &= \Pr[\log_2(1+\gamma_{r1,d}) > T_d] \\ &= \Pr[|h_{s1}|^2 > \frac{(2^{T_d}-1)\,\sigma^2}{P_s(1-\alpha\,2^{T_d})}], \\ &= \exp(-\frac{\left(2^{T_d}-1\right)\,\sigma^2}{(1-\alpha\,2^{T_d})P_s\,\lambda}), \qquad (26)\\ \Pr[A_2^c] &= \Pr[\frac{1}{3}\,\log_2(1+\gamma_{r1}) > T_r] \\ &= \Pr[|h_{s1}|^2 > \frac{\left(2^{3\,T_r}-1\right)\,\sigma^2}{\alpha\,P_s}] \\ &= \exp(-\frac{(2^{3\,T_r}-1)\,\sigma^2}{\alpha\,P_s\,\lambda}). \qquad (27)\end{aligned}$$

By substituting (26) and (27) into (25), the closed-form expression for outage probability of R_1 in (12) is obtained. On the other hand, the outage probability of R_2 is given by

$$\mathcal{O}_{R_2} = 1 - \Pr[B_1^c]\,\Pr[B_2^c].$$

Given $|h_{s2}|^2 \sim \mathcal{CN}(0,\,\lambda)$ and $|h_{s1}|^2 \sim \mathcal{CN}(0,\,\lambda)$ are independent and identically distributed, thus, $\Pr[B_1^c] = \Pr[A_1^c]$ and $\Pr[B_2^c] = \Pr[A_2^c]$. Therefore, $\Pr[\mathcal{O}_{R_2}] = \Pr[\mathcal{O}_{R_1}]$ and Theorem 1 is obtained.

B. PROOF OF THEOREM 2

Given the probability that D can decode $x_d(t_1)$ from R_1 successfully and D can decode $x_d(t_2)$ from R_2 successfully are

$$\begin{aligned}&\Pr[\min(\gamma_{r1,d},\,\gamma_{d1}) > 2^{3\,T_d}-1] \\ &\quad= \exp(-\frac{\left(2^{3\,T_d}-1\right)\,\sigma^2}{(1-\alpha\,2^{3\,T_d})P_s\,\lambda} - \frac{\left(2^{3\,T_d}-1\right)\,\sigma^2}{P_r\,\lambda}), \qquad (28)\end{aligned}$$

and

$$\begin{aligned}&\Pr[\min(\gamma_{r2,d},\,\gamma_{d2}) > 2^{3\,T_d}-1] \\ &\quad= \exp(-\frac{\left(2^{3\,T_d}-1\right)\,\sigma^2}{(1-\alpha\,2^{3\,T_d})P_s\,\lambda} - \frac{\left(2^{3\,T_d}-1\right)\,\sigma^2}{P_r\,\lambda}), \qquad (29)\end{aligned}$$

respectively. The outage probability of D is given by

$$\begin{aligned}\mathcal{O}_D = 1 &- \Pr[\min(\gamma_{r1,d},\,\gamma_{d1}) > 2^{3\,T_d}-1] \\ &\times \Pr[\min(\gamma_{r2,d},\,\gamma_{d2}) > 2^{3\,T_d}-1]. \qquad (30)\end{aligned}$$

By substituting (28) and (29) into (30), the closed-form expression for outage probability of D in (14) is obtained.

C. PROOF OF THEOREM 3

A closed-form expression for ergodic rate of R_1 is given by

$$\begin{aligned}\overline{C}_{R_1} &= \mathrm{E}[\frac{1}{3}\,\log_2(1+\gamma_{r1})] \\ &= \frac{1}{3\,\ln 2}\int_0^\infty \frac{1-F_{\gamma_{r1}}(x)}{1+x}\,dx \\ &\overset{(a)}{=} -\frac{1}{3\,\ln 2}\,\exp\left(\frac{\sigma^2}{\alpha\,P_s\,\lambda}\right)\mathrm{Ei}\left(-\frac{\sigma^2}{\alpha\,P_s\,\lambda}\right),\end{aligned}$$

where $F_{\gamma_{r1}}(x) = 1 - \exp\left(-\frac{\sigma^2 x}{\alpha\,P_s\,\lambda}\right)$, (a) follows [18, eq. (3.352.4)], and $\mathrm{E}[X]$ denotes expectation of a random variable X. Given $F_{\gamma_{r2}}(x) = F_{\gamma_{r1}}(x)$, therefore, $\overline{C}_{R_2} = \overline{C}_{R_1}$ and Theorem 3 in (21) is obtained.

D. PROOF OF THEOREM 4

A closed-form expression for ergodic rate of D is not obtainable. Alternately, an asymptotic ergodic rate of D at high SNR is achievable. At high SNR regime, the instantaneous achievable rate in (20) can be written as

$$\begin{aligned}C_D &\approx \frac{2}{3}\,\log_2(1+\frac{\beta\,P_s\,\min\left\{|h_{s1}|^2,\,|h_{s2}|^2\right\}}{\alpha\,P_s\,\min\left\{|h_{s1}|^2,\,|h_{s2}|^2\right\}+\sigma^2}) \\ &\approx \frac{2}{3}\,\left\{\log_2(1+\frac{P_s}{\sigma^2}\,\min\left\{|h_{s1}|^2,\,|h_{s2}|^2\right\}) \right. \\ &\quad \left. -\log_2(1+\frac{\alpha\,P_s}{\sigma^2}\,\min\left\{|h_{s1}|^2,\,|h_{s2}|^2\right\})\right\}. \qquad (31)\end{aligned}$$

Given the PDF of $Y_2 = \min\left\{|h_{s1}|^2,\,|h_{s2}|^2\right\}$ is $f_{Y_2}(x) = \frac{2}{\lambda}\,\exp\left(-\frac{2x}{\lambda}\right)$ and the asymptotic ergodic rate of D is

$$\begin{aligned}\overline{C}_D &\approx \mathrm{E}[C_D] \\ &\approx \frac{2}{3}\,\left\{\int_0^\infty \log_2(1+\frac{P_s\,x}{\sigma^2})f_{Y_2}(x)\,dx \right. \\ &\quad \left. -\int_0^\infty \log_2(1+\frac{\alpha\,P_s\,x}{\sigma^2})f_{Y_2}(x)\,dx\right\}. \qquad (32)\end{aligned}$$

Using $\log_2(x) = \ln(x)\,\log_2(\exp(1))$ and [18, eq. (4.337.2)],

$$\begin{aligned}&\int_0^\infty \log_2(1+\frac{P_s\,x}{\sigma^2})f_{Y_2}(x)\,dx \\ &\qquad = -\log_2(\exp(1))\,\exp\left(\frac{2\,\sigma^2}{P_s\,\lambda}\right)\mathrm{Ei}\left(-\frac{2\,\sigma^2}{P_s\,\lambda}\right), \qquad (33)\end{aligned}$$

and

$$\begin{aligned}&\int_0^\infty \log_2(1+\frac{\alpha\,P_s\,x}{\sigma^2})f_{Y_2}(x)\,dx \\ &\qquad = -\log_2(\exp(1))\,\exp\left(\frac{2\,\sigma^2}{\alpha\,P_s\,\lambda}\right)\mathrm{Ei}\left(-\frac{2\,\sigma^2}{\alpha\,P_s\,\lambda}\right). \qquad (34)\end{aligned}$$

Theorem 4 is obtained by substituting (33) and (34) into (32).

E. DESCRIPTIONS OF COMPARABLE SCHEMES

In HD-NOMA and FD-NOMA, *BS* broadcasts $x_s(t_1)$ in (1) and $x_s(t_2)$ in (5) to R in two different time slots. After receiving $x_s(t_j)$, R decodes $x_r(t_1)$ and $x_d(t_j)$ using SIC technique, where $j = \{1,\,2\}$. Then, R relays the decoded $x_d(t_j)$ to D. In HD-NOMA, R operates in HD mode, i.e., R cannot transmit and receive signals simultaneously. Therefore, *BS* needs to stop transmitting for one time slot when R relays previous decoded message to D. Meanwhile, in FD-NOMA, R operates in FD mode, i.e., R can transmit and receive

TABLE 4. Transmission of HD-NOMA and FD-NOMA.

	HD-NOMA		FD-NOMA	
Time Slots	BS	R	BS	R
1	$x_s(t_1)$	-	$x_s(t_1)$	$x_d(t_1)$
2	-	$x_d(t_1)$	$x_s(t_2)$	$x_d(t_2)$
3	$x_s(t_2)$	-		
4	-	$x_d(t_2)$		

TABLE 5. Transmission of HD-OMA and FD-OMA.

	HD-OMA		FD-OMA	
Time Slots	BS	R	BS	R
1	$x_r(t_1)$	-	$x_r(t_1)$	-
2	$x_r(t_2)$	-	$x_r(t_2)$	-
3	$x_d(t_1)$	-	$x_d(t_1)$	$x_d(t_1)$
4	-	$x_d(t_1)$	$x_d(t_2)$	$x_d(t_2)$
5	$x_d(t_2)$	-		
6	-	$x_d(t_2)$		

TABLE 6. SINR and SNR of HD-NOMA and FD-NOMA.

	HD-NOMA	FD-NOMA
$\gamma_{R,d}$	$\frac{\beta P_s\lvert h_{sr}\rvert^2}{\alpha P_s\lvert h_{sr}\rvert^2+\sigma^2}$	$\frac{\beta P_s\lvert h_{sr}\rvert^2}{\alpha P_s\lvert h_{sr}\rvert^2+K P_r\lvert h_{FD}\rvert^2+\sigma^2}$
γ_R	$\frac{\alpha P_s\lvert h_{sr}\rvert^2}{\sigma^2}$	$\frac{\alpha P_s\lvert h_{sr}\rvert^2}{K P_r\lvert h_{FD}\rvert^2+\sigma^2}$

TABLE 7. SINR and SNR of HD-OMA and FD-OMA.

	HD-OMA	FD-OMA
γ_{oR}	$\frac{P_{s,o}\lvert h_{sr}\rvert^2}{\sigma^2}$	$\frac{P_{s,o}\lvert h_{sr}\rvert^2}{K P_r\lvert h_{FD}\rvert^2+\sigma^2}$

signals simultaneously. The transmission of HD-NOMA and FD-NOMA are shown in Table 4.

On the other hand, in HD-OMA and FD-OMA, BS broadcasts $x_r(t_1)$, $x_r(t_2)$, $x_d(t_1)$, and $x_d(t_2)$ in orthogonal time slots, i.e., time division multiple access (TDMA). In HD-OMA, D needs four time slots to receive $x_d(t_1)$ and $x_d(t_2)$ and two more time slots are needed for R to receive $x_r(t_1)$ and $x_r(t_2)$. Meanwhile, in FD-OMA, D needs two time slots only to receive $x_d(t_1)$ and $x_d(t_2)$, because R operates in FD mode. The transmission of HD-OMA and FD-OMA are shown in Table 5.

1) SINR AND SNR OF COMPARABLE SCHEMES

Based on SIC technique, the SINR and SNR of HD-NOMA and FD-NOMA when R decodes $x_d(t_j)$ and $x_r(t_j)$, i.e., $\gamma_{R,d}$ and γ_R, are listed in Table 6, where $h_{sr} \sim \mathcal{CN}(0, \lambda)$ and $h_{FD} \sim \mathcal{CN}(0, \lambda)$ denote the channel between BS and R and self-interference channel, respectively. $K P_r |h_{FD}|^2$ is the residual self-interference [9], where K is self-interference cancellation factor and P_r is transmission power of R. On the other hand, the received SNR at R in HD-OMA and FD-OMA, γ_{oR} are listed in Table 7, where $P_{s,o} = P_s/2$ is the transmission power of BS in HD-OMA and FD-OMA. Meanwhile, the SNR of HD-NOMA, FD-NOMA, HD-OMA, and FD-OMA when D decodes $x_d(t_j)$ from R are

$$\gamma_d = \frac{P_r\,|h_{rd}|^2}{\sigma^2}, \tag{35}$$

where $h_{rd} \sim \mathcal{CN}(0, \lambda)$ denotes the channel between R and D.

2) OUTAGE PROBABILITY OF COMPARABLE SCHEMES

For HD-NOMA and FD-NOMA, outage probability of each stream at R and D are

$$\mathcal{O}_R = 1 - \Pr\left[\log_2(1+\gamma_{R,d}) \geq T_d\right] \times \Pr\left[\frac{1}{TS}\log_2(1+\gamma_R) \geq T_r\right], \tag{36}$$

and

$$\mathcal{O}_D = 1 - \Pr\left[\frac{1}{TS}\log_2(1+\min\left(\gamma_{R,d},\,\gamma_d\right)) \geq T_d\right], \tag{37}$$

respectively, where TS is the required time slots for a complete transmission. TS of HD-NOMA and FD-NOMA are 4 and 2, respectively, as given in Table 4. Meanwhile, for HD-OMA and FD-OMA, outage probability of each stream at R and D are

$$\mathcal{O}_{O,R} = 1 - \Pr\left[\frac{1}{TS}\log_2(1+\gamma_{oR}) \geq T_r\right], \tag{38}$$

and

$$\mathcal{O}_{O,D} = 1 - \Pr[\frac{1}{TS}\log_2(1+\min\left(\gamma_{oR},\,\gamma_d\right)) \geq T_d], \tag{39}$$

where TS of HD-OMA and FD-OMA are 6 and 4, respectively, as given in Table 5.

3) INSTANTANEOUS SUM RATE OF COMPARABLE SCHEMES

The instantaneous sum rate of the cooperative NOMA system, i.e., HD-NOMA and FD-NOMA, and cooperative OMA system, i.e., HD-OMA and FD-OMA, are

$$C_{NOMA} = \frac{2}{TS}\log_2(1+\gamma_R) + \frac{2}{TS}\log_2(1+\min\left(\gamma_{R,d},\,\gamma_d\right)), \tag{40}$$

$$C_{OMA} = \frac{2}{TS}\log_2(1+\gamma_{oR}) + \frac{2}{TS}\log_2(1+\min\left(\gamma_{oR},\,\gamma_d\right)), \tag{41}$$

respectively.

REFERENCES

[1] J. G. Andrews *et al.*, "What will 5G be?" *IEEE J. Sel. Areas Commun.*, vol. 32, no. 6, pp. 1065–1082, Jun. 2014.
[2] F. Boccardi, R. W. Heath, Jr., A. Lozano, T. L. Marzetta, and P. Popovski, "Five disruptive technology directions for 5G," *IEEE Commun. Mag.*, vol. 52, no. 2, pp. 74–80, Feb. 2014.
[3] Y. Saito, A. Benjebbour, Y. Kishiyama, and T. Nakamura, "System-level performance evaluation of downlink non-orthogonal multiple access (NOMA)," in *Proc. IEEE Int. Symp. Pers., Indoor Mobile Radio Commun. (PIMRC)*, London, U.K., Sep. 2013, pp. 611–615.
[4] Z. Ding, Z. Yang, P. Fan, and H. V. Poor, "On the performance of non-orthogonal multiple access in 5G systems with randomly deployed users," *IEEE Signal Process. Lett.*, vol. 21, no. 12, pp. 1501–1505, Dec. 2014.
[5] Z. Ding, M. Peng, and H. V. Poor, "Cooperative non-orthogonal multiple access in 5G systems," *IEEE Commun. Lett.*, vol. 19, no. 8, pp. 1462–1465, Aug. 2015.
[6] J.-B. Kim and I.-H. Lee, "Capacity analysis of cooperative relaying systems using non-orthogonal multiple access," *IEEE Commun. Lett.*, vol. 19, no. 11, pp. 1949–1952, Nov. 2015.

[7] J.-B. Kim and I.-H. Lee, "Non-orthogonal multiple access in coordinated direct and relay transmission," *IEEE Commun. Lett.*, vol. 19, no. 11, pp. 2037–2040, Nov. 2015.
[8] Z. Zhang, Z. Ma, M. Xiao, Z. Ding, and P. Fan, "Full-duplex device-to-device aided cooperative non-orthogonal multiple access," *IEEE Trans. Veh. Technol.*, vol. 66, no. 5, pp. 4467–4471, May 2017.
[9] L. Zhang, J. Liu, M. Xiao, G. Wu, Y.-C. Liang, and S. Li, "Performance analysis and optimization in downlink NOMA systems with cooperative full-duplex relaying," *IEEE J. Sel. Areas Commun.*, vol. 35, no. 10, pp. 2398–2412, Oct. 2017.
[10] X. Yue, Y. Liu, S. Kang, A. Nallanathan, and Z. Ding, "Exploiting full/half-duplex user relaying in NOMA systems," *IEEE Trans. Commun.*, vol. 66, no. 2, pp. 560–575, Feb. 2017.
[11] Z. Zhang, K. Long, A. V. Vasilakos, and L. Hanzo, "Full-duplex wireless communications: Challenges, solutions, and future research directions," *Proc. IEEE*, vol. 104, no. 7, pp. 1369–1409, Jul. 2016.
[12] S.-N. Hong and G. Caire, "Virtual full-duplex relaying with half-duplex relays," *IEEE Trans. Inf. Theory*, vol. 61, no. 9, pp. 4700–4720, Sep. 2015.
[13] B. Rankov and A. Wittneben, "Spectral efficient protocols for half-duplex fading relay channels," *IEEE J. Sel. Areas Commun.*, vol. 25, no. 2, pp. 379–389, Feb. 2007.
[14] Q. Y. Liau, C. Y. Leow, and Z. Ding, "Amplify-and-forward virtual full-duplex relaying-based cooperative NOMA," *IEEE Wireless Commun. Lett.*, vol. 7, no. 3, pp. 464–467, Jun. 2018.
[15] Z. Ding, P. Fan, and H. V. Poor, "Impact of user pairing on 5G non-orthogonal multiple access downlink transmissions," *IEEE Trans. Veh. Technol.*, vol. 65, no. 8, pp. 6010–6023, Aug. 2016.
[16] X. Yue, Y. Liu, S. Kang, A. Nallanathan, and Y. Chen, "Modeling and analysis of two-way relay non-orthogonal multiple access systems," *IEEE Trans. Commun.*, vol. 66, no. 9, pp. 3784–3796, Sep. 2018.
[17] L. Zheng and D. N. C. Tse, "Diversity and multiplexing: A fundamental tradeoff in multiple-antenna channels," *IEEE Trans. Inf. Theory*, vol. 49, no. 5, pp. 1073–1096, May 2003.
[18] I. S. Gradshteyn and I. M. Ryžhik, *Table of Integrals, Series, and Products*, 7th ed. Amsterdam, The Netherlands: Elsevier, 2007.
[19] H. Ju, E. Oh, and D. Hong, "Improving efficiency of resource usage in two-hop full duplex relay systems based on resource sharing and interference cancellation," *IEEE Trans. Wireless Commun.*, vol. 8, no. 8, pp. 3933–3938, Aug. 2009.

QIAN YU LIAU received the B.Eng. degree in electrical-telecommunications and the M.Sc. degree in electrical from Universiti Teknologi Malaysia, Johor Bahru, Malaysia, in 2013 and 2016, respectively, where she is currently pursuing the Ph.D. degree in wireless communications. Her research interests include wireless relaying, physical layer security, and non-orthogonal multiple access.

CHEE YEN LEOW (S'08–M'12) received the B.Eng. degree in computer engineering from Universiti Teknologi Malaysia (UTM), Johor Bahru, Malaysia, in 2007, and the Ph.D. degree from Imperial College London, U.K., in 2011. Since 2007, he has been an Academic Staff with the School of Electrical Engineering, Faculty of Engineering, UTM. He is currently an Associate Professor with the Faculty and a Research Fellow with the Wireless Communication Centre, the Higher Institution Centre of Excellence, UTM, and the UTM-Ericsson Innovation Centre for 5G. His research interests include non-orthogonal multiple access, cooperative communication, UAV communication, MIMO, hybrid beamforming, physical layer security, wireless power transfer, convex optimization, game theory, and prototype development using software defined radio, for 5G and IoT applications.